BODY EFFECT ON WING ANGLE OF ATTACK AND PITCHING MOMENT AT ZERO LIFT AT LOW SPEEDS

1. NOTATION AND UNITS (see Sketch 1.1)

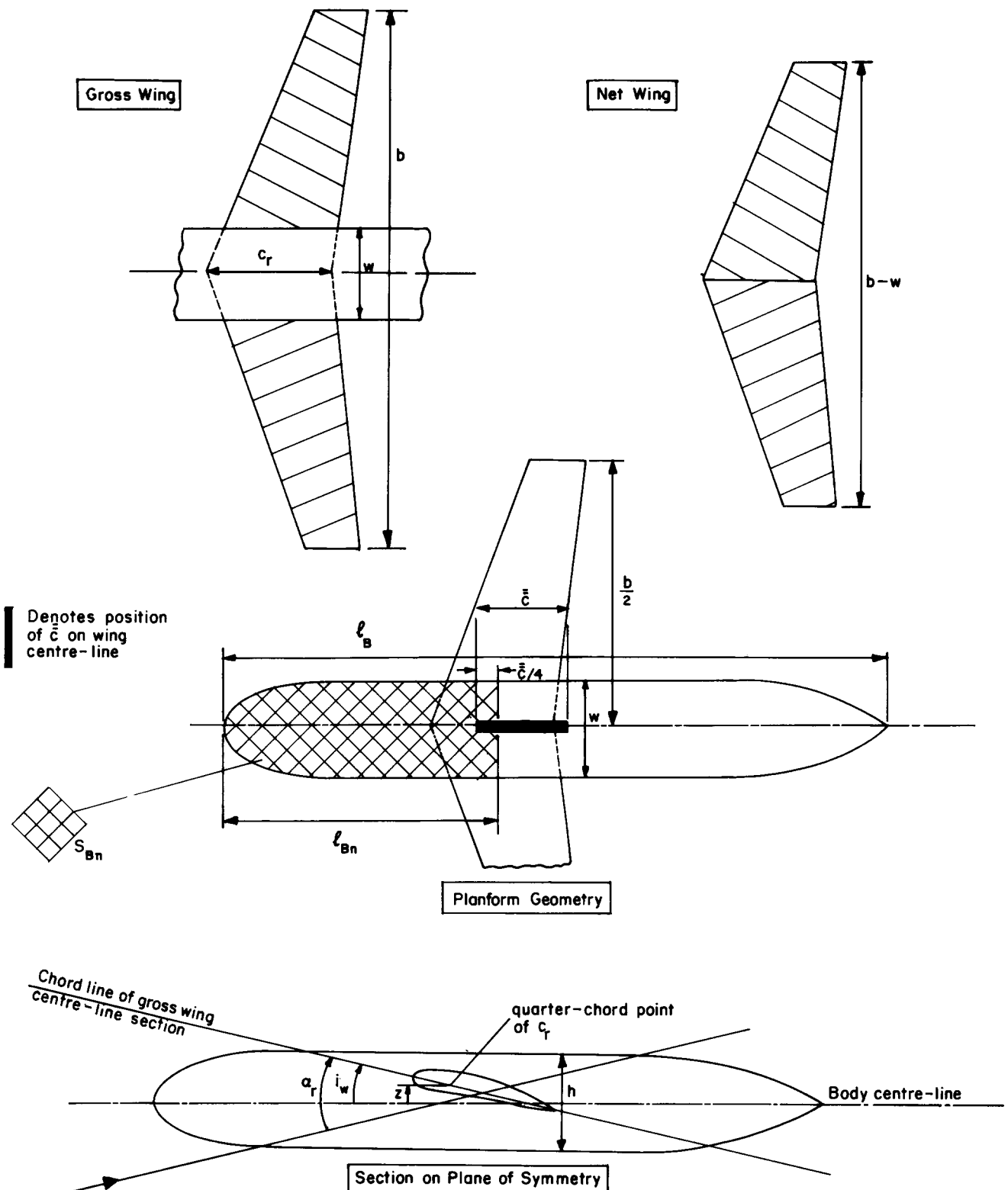|		*SI*	*British*
A	aspect ratio of gross wing		
a_{1N}	lift-curve slope of net wing based on qS_N (from Item No. 70011, Derivation 15)	rad^{-1}	rad^{-1}
a_{1WB}	lift-curve slope of wing-body combination based on qS_W	rad^{-1}	rad^{-1}
b	span of gross wing	m	ft
C_{LW}	lift coefficient of gross wing based on qS_W		
C_{LWB}	lift coefficient of wing-body combination based on qS_W		
$\Delta_z C_{LWB}$	increment in C_{LWB} due to vertical displacement of wing from mid-body position		
C_{mW}	pitching moment coefficient of gross wing about quarter-chord point of $\bar{\bar{c}}$ and based on $qS_W\bar{\bar{c}}$		
C_{m0W}	pitching moment coefficient of gross wing at $C_{LW} = 0$ (from experiment or Item No. 87001, Derivation 20)		
$(C_{m0})_B$	increment in C_{m0W} due to body for unswept wing ($\Lambda_{1/4} = 0$) at mid-body height		
C_{m0WB}	pitching moment coefficient of wing-body combination at $C_{LWB} = 0$		
ΔC_{m0}	increment in C_{m0W} due to adding body, ($= C_{m0WB} - C_{m0W}$)		
$\Delta_s C_{m0}$	increment in $(C_{m0})_B$ due to sweepback of wing		
$\Delta_z C_{m0}$	increment in $(C_{m0})_B$ due to vertical displacement of wing from mid-body position		
$\bar{\bar{c}}$	aerodynamic mean chord of gross wing	m	ft
c_r	centre-line chord of gross wing	m	ft
h	maximum height of body	m	ft
i_W	angle between chord line of gross wing centre-line section and centre-line of body	rad*	rad*

For footnote refer to end of Notation.

K_1, K_2	slender-body theory factors in Equations (3.1) to (3.3)		
l_B	length of body	m	ft
l_{Bn}	distance from body nose to quarter-chord point of $\bar{\bar{c}}$	m	ft
q	kinetic pressure	N/m^2	lbf/ft^2
S_B	planform area of body	m^2	ft^2
S_{Bn}	planform area of body forward of lateral line through quarter-chord point of $\bar{\bar{c}}$	m^2	ft^2
S_N	planform area of net wing	m^2	ft^2
S_W	planform area of gross wing	m^2	ft^2
w	maximum width of body	m	ft
z	vertical displacement of quarter-chord point of c_r above mid-body position, positive for high wing	m	ft
α_r	angle of attack of chord line of gross wing centre-line section	rad	rad
α_{0rW}	value of α_r for $C_{LW} = 0$ (from experiment or Item No. 87031, Derivation 21)	rad*	rad*
$(\alpha_{0r})_1$	contribution to α_{0rW} due to camber alone (from Item No. 87031, Derivation 21)	rad*	rad*
α_{0rWB}	value of α_r for wing-body combination for $C_{LWB} = 0$	rad*	rad*
$\Delta\alpha_{0r}$	$\alpha_{0rWB} - \alpha_{0rW}$, (see Sketch 3.1)	rad*	rad*
δ_t	geometric twist of wing tip relative to centre-line chord of gross wing, positive leading-edge up	deg	deg
$\Lambda_{1/4}$	sweepback of wing quarter-chord line	deg	deg
λ	taper ratio of gross wing		
ϕ_a, ϕ_f	afterbody, forebody sweep angles as defined in Sketch 4.1	deg	deg
ψ	angle between zero-lift plane of wing and airflow direction for zero body-alone pitching moment	deg	deg

Subscripts

expt	denotes experimental value
pred	denotes predicted value

---

* N.B. In the final application the angles (rad*) in Equations (3.5) and (3.6) may be conveniently converted into degrees.
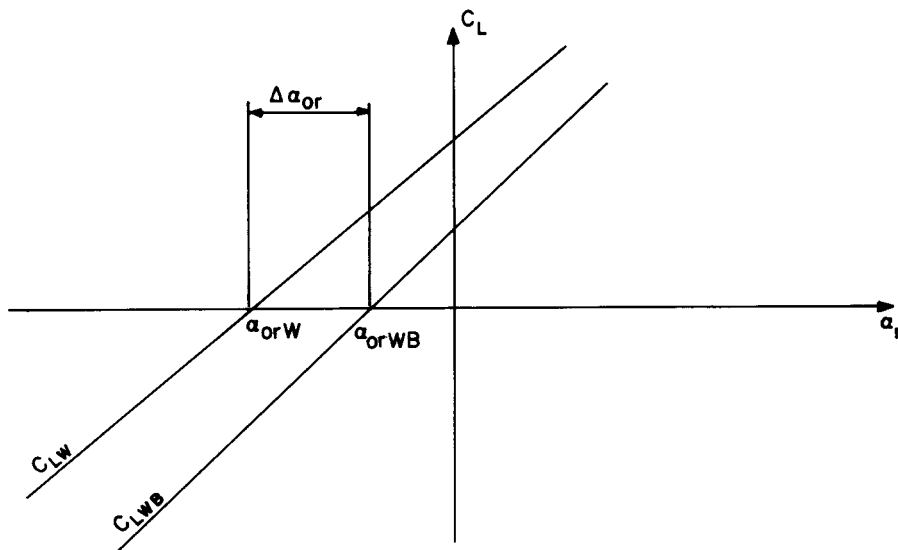
Sketch 1.1   Definition of geometry

2. INTRODUCTION

This Item provides simple, mostly empirical, methods for estimating the change of zero-lift angle of attack and pitching-moment coefficient for a wing due to adding a fuselage of circular or approximately circular cross-section. The method for zero-lift angle of attack is presented in Section 3, and is an adaptation of a formula from Derivation 17. The method for zero-lift pitching-moment coefficient is presented in Section 4, and is based on the predictions of Derivation 2 for unswept wings on axisymmetric bodies, with additional empirical allowance for wing sweep and body asymmetry. The effects of Mach number and Reynolds number are discussed in Section 5. The applicability and accuracy of the methods are given in Section 6. The Derivation is listed in Section 7, and Section 8 provides a worked example.

3. ZERO-LIFT ANGLE OF ATTACK

Sketch 3.1   Lift coefficient curves

In inviscid flow the force on a closed body at angle of attack is zero. However, in viscous flow the force is found to be finite, due largely to the boundary layer on the afterbody. This, combined with aerodynamic interference of the wing and body, gives rise to a change of lift and zero-lift angle of attack when a body is attached to a wing. An axisymmetric body attached to an uncambered, untwisted wing with zero setting angle, and with the wing on the centre-line of the body, should preserve symmetry so that $\alpha_{0rW} = \alpha_{0rWB} = 0$.

The lift on the body is affected by the upwash and downwash due to the wing and vice versa. The crossflow around the body induces a change in the angles of attack of the wing sections, particularly near the wing-body junction. In addition, vertical displacement of the wing further complicates the flow pattern.

Because these effects are greatly influenced by viscosity they are difficult to predict. However, Derivation 17 gives the following expression to estimate the total lift of a wing-body combination for circular section bodies, with wing-body interference effects for mid-wings estimated via slender-body theory as set out in Derivation 13, and with an empirical allowance for wing height from Derivation 14:

$$C_{LWB} = K_1 a_{1N} \left\{ [\alpha_r - i_W - \alpha_{0rW} + (\alpha_{0r})_1] + \frac{K_2}{K_1}[i_W - (\alpha_{0r})_1] \right\} + \Delta_z C_{LWB}, \quad (3.1)$$

where $\quad K_1 = \dfrac{a_{1WB}}{a_{1N}}$ and $K_2 = \dfrac{1}{a_{1N}}\left(\dfrac{\partial C_{LWB}}{\partial i_W}\right)$ for constant body angle of attack.

Derivation 17 gives the following numerical approximations to the slender-body values of K_1 and K_2 for $w/b \le 0.2$,

$$K_1 = \left(1 + 2.15\frac{w}{b}\right)\frac{S_N}{S_W} + \frac{\pi}{2a_{1N}}\frac{w^2}{S_N}\frac{S_N}{S_W} \quad (3.2)$$

and $\quad K_2 = \left(1 + 0.7\frac{w}{b}\right)\frac{S_N}{S_W}.$ $\qquad (3.3)$

From Derivation 14 there is the empirical approximation, for $w/b \approx 0.1$,

$$\Delta_z C_{LWB} = -0.2c_r w(z/h)/S_W, \quad (3.4)$$

where a linear variation with z/h has been assumed between values of $\pm 0.1 c_r w/S_W$ quoted for "low" or "high" wings, respectively.

Rearrangement of Equation (3.1) with $C_{LWB} = 0$ allows formulae for α_{0rWB} and $\Delta\alpha_{0r}$ to be developed. However, comparisons with experimental data have established that wing height has only a minor influence on those parameters and that a simpler prediction method of comparable accuracy can be produced if the small contribution $\Delta_z C_{LWB}$ is omitted from Equation (3.1) before rearrangement.

With $C_{LWB} = \Delta_z C_{LWB} = 0$, Equation (3.1) can be rewritten to give

$$\alpha_r = \alpha_{0rWB} = \alpha_{0rW} + \left[1 - \frac{K_2}{K_1}\right]\left[i_W - (\alpha_{0r})_1\right], \quad (3.5)$$

and hence $\quad \Delta\alpha_{0r} = \alpha_{0rWB} - \alpha_{0rW} = \left[1 - \dfrac{K_2}{K_1}\right]\left[i_W - (\alpha_{0r})_1\right].$ $\qquad (3.6)$

Values of α_{0rW} and $(\alpha_{0r})_1$ may be calculated by the method of Item No. 87031 (Derivation 21), see Section 8 for example. If experimental values of α_{0rW} are available then they may be substituted instead.

With the term due to $\Delta_z C_{LWB}$ already neglected, the necessity to calculate a_{1N} is completely avoided, without unacceptable loss of accuracy, by taking a typical value of $\pi w^2/(2a_{1N}S_N) = 0.03$ and so writing

$$K_1 = \left(1.03 + 2.15\frac{w}{b}\right)\frac{S_N}{S_W} \quad (3.7)$$

so that
$$\frac{K_2}{K_1} = \frac{(1 + 0.7w/b)}{(1.03 + 2.15w/b)}. \tag{3.8}$$

Figure 1 gives K_2/K_1 as a function of w/b.

4. ZERO-LIFT PITCHING-MOMENT COEFFICIENT

The change in zero-lift pitching-moment coefficient ΔC_{m0} due to adding a body to a wing is, for similar reasons to those discussed earlier for angle of attack, difficult to predict with precision. Although the pitching moments for the body and wing can be estimated separately, the complex flow around a wing-body combination precludes a simple addition.

Derivation 2 gives an empirical method for estimating the change in zero-lift pitching-moment coefficient due to adding an axisymmetric body to an unswept wing. The contribution $(C_{m0})_B$ for a wing mounted at mid-body height is obtained from Figure 2, (from Derivation 2). A further term $\Delta_z C_{m0}$ accounts for wing height on the body, and the result in Derivation 2 has been generalised herein by the assumption of a linear variation with z/h. Accounting for wing sweep is theoretically difficult but a simple increment $\Delta_s C_{m0}$ calculated from the twist, aspect ratio and sweep of the quarter-chord line is proposed.

Thus
$$\begin{aligned} C_{m0WB} &= C_{m0W} + \Delta C_{m0} \\ &= C_{m0W} + (C_{m0})_B + \Delta_z C_{m0} + \Delta_s C_{m0} \end{aligned} \tag{4.1}$$

where the wing-alone value C_{m0W} may be found by the method of Item No. 87001 (Derivation 20), see Section 8 for example. If experimental values of C_{m0W} are available then they may be substituted instead.

With $(C_{m0})_B$ obtained from Figure 2, the remaining components of ΔC_{m0} are

$$\Delta_z C_{m0} = 0.01(z/h), \tag{4.2}$$

and
$$\Delta_s C_{m0} = -0.053[(C_{m0})_B \delta_t (w/b) A \tan \Lambda_{\frac{1}{4}}]^{0.3}, \text{ where } \delta_t \text{ is in degrees.} \tag{4.3}$$

Note that Equation (4.3) has been developed for configurations with $\delta_t \le 0$ and $\Lambda_{\frac{1}{4}} \ge 0$, and should not be employed otherwise.

To evaluate $(C_{m0})_B$ from Figure 2, the angle between the zero-lift plane of the wing and the airflow direction for zero body-alone pitching moment ψ (in degrees) is required. For axisymmetric bodies, with i_W and α_{0rW} in degrees, this is obtained as

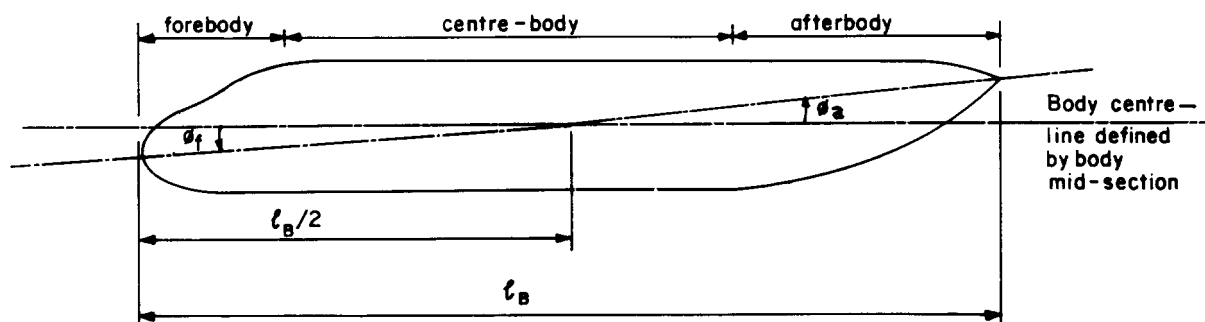$$\psi = i_W - \alpha_{0rW}. \tag{4.4}$$

However, for downswept forebodies or upswept afterbodies or any other asymmetries, it is more difficult to define ψ unless experimental data are known for the body alone. In the absence of body-alone data, analysis of the few data available from compatible wing-body and wing-alone tests suggests that the following estimate may be used

$$\psi = i_W - \alpha_{0rW} + \phi_f - 0.6\phi_a, \tag{4.5}$$

with ϕ_f and ϕ_a defined as in Sketch 4.1. Equation (4.5) must be regarded only as an ad hoc solution to the

estimation of ψ and should be employed only for bodies similar to those studied in the preparation of this Item, where the forebody downsweep is limited to a length of about one body diameter, the afterbody upsweep to a length of three or four body diameters and the centre-body to a length of four or more body diameters. For less conventional configurations the estimate provided may be unsatisfactory.

Sketch 4.1   Body sweep angles ϕ_a , ϕ_f

5.   EFFECT OF MACH NUMBER AND REYNOLDS NUMBER

It might be expected that, since much of the flow around the wing-body combination is at least partially governed by viscous effects, Reynolds number would be an important parameter in determining α_{0rWB} and C_{m0WB}. Experimental data (Derivations 1, 3, 5 to 10, 19 and 22) are inconclusive in their trends, but the effects of Reynolds number based on $\bar{\bar{c}}$ over the range 0.5×10^6 to 5×10^6 are small overall.

Similarly, compressibility effects appear to be unimportant for Mach numbers up to 0.4 at least.

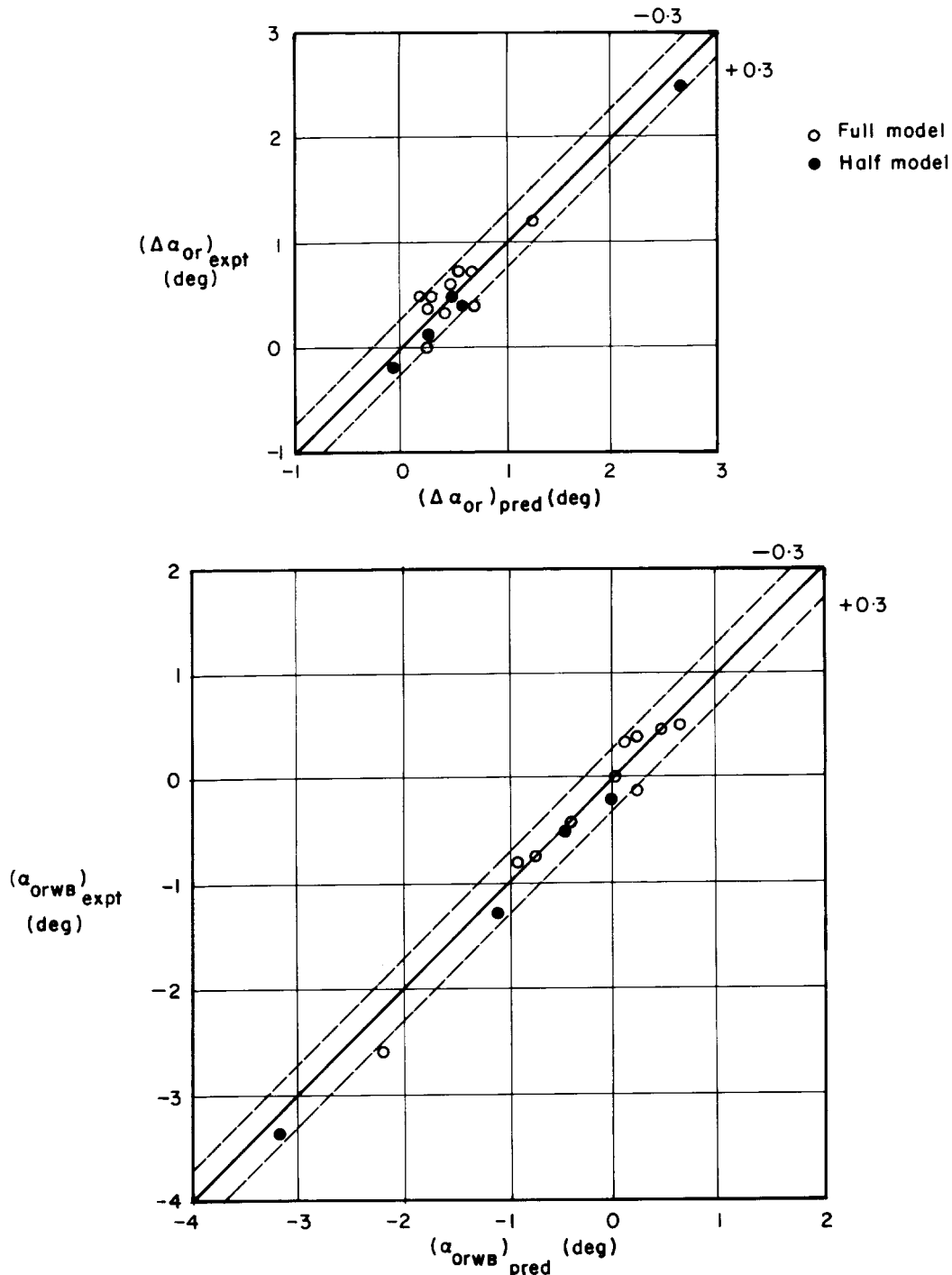## 6.   APPLICABILITY AND ACCURACY

The methods of this Item work well for wing-body combinations with closed bodies of nearly circular cross-section. They must not be applied to bodies with square or rectangular cross-sections as they can then give rise to unacceptably large errors in both $\Delta\alpha_{0r}$ and ΔC_{m0} (Derivations 11 and 12). Body profile does not influence $\Delta\alpha_{0r}$ noticeably, but the calculation of ΔC_{m0} for non-axisymmetric bodies must be treated with caution because of uncertainties introduced through the definition of ψ, see comments following Equation (4.5). The presence of wing-root fillets can influence C_{m0}, but the magnitude of the effect is crucially dependent on the detailed geometry of individual configurations and therefore best determined via model testing. An empirical first approximation to the contribution from trailing-edge fillets can be made by the method of Derivation 4, although it is restricted to a limited range of fillet geometries that may not always be representative of current practice.

Although they are formally defined in radians, the angles α_{0rWB}, α_{0rW}, i_W and $(\alpha_{0r})_1$ may, for convenience, all be measured in degrees in Equations (3.5) and (3.6).
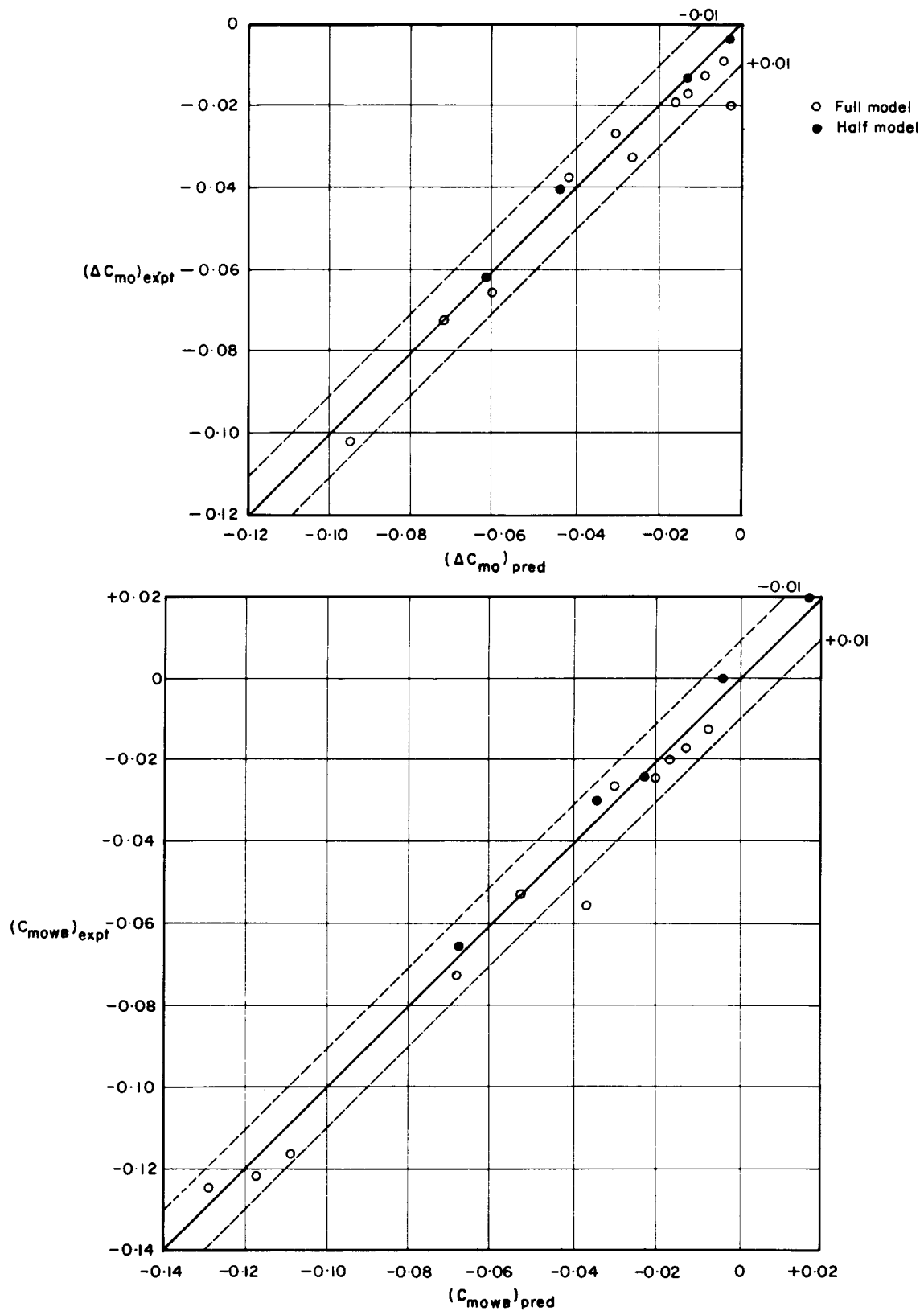
When, as will normally be the case, the methods of Item Nos 87031 and 87001 are used to predict α_{0rW} and C_{m0W} respectively, the limitations on the applicability of those Items should be observed. It should be noted that both of those Items require the estimation of approximate theoretical two-dimensional zero-lift characteristics by the methods of Item No. 74024 (Derivation 16). If the gross wing planform is not straight-tapered then Item Nos 87031 and 87001 advise that the geometric construction described in Item No. 76003 (Derivation 18) be used to produce an "equivalent" wing planform of straight taper and so obtain any necessary values of wing planform parameters. The same approach should be used to obtain a gross

wing planform for use in this Item. The angle i_W, the section camber-line shape and the spanwise twist distribution remain as for the true wing. See Section 8 for example.

The assessment of the accuracy of the methods in this Item has been made using experimental values of α_{0rW} and C_{m0W} for the wing alone, so confining any errors to the effect of adding the body. On this basis, $\Delta\alpha_{0r}$ and α_{0rWB} are predicted to within about $\pm 0.3°$, see Sketch 6.1, and ΔC_{m0} and C_{m0WB} to within about ± 0.01, see Sketch 6.2. The lowest wing aspect ratio considered was $A = 3$ and the method is not recommended for lower values. Data from tests on half models were found to be predicted with comparable accuracy to those from full-model tests.

Sketch 6.1   Comparison of experimental and predicted values

Sketch 6.2   Comparison of experimental and predicted values

7. DERIVATION

The Derivation lists the sources that have assisted in the preparation of this Item.

1. SALMI, R.J.
CONNOR, D.W.
GRAHAM, R.R.
Effects of fuselage on the aerodynamic characteristics of a 42° sweptback wing at Reynolds numbers to 8,000,000. NACA RM L7E13 (TIL 1185), 1947.

2. RAeS
Royal Aeronautical Society tech. Note No. 3, unpublished, 1949.

3. SIVELLS, J.C.
SPOONER, S.H.
Investigation in the Langley 19 foot pressure tunnel of two wings of NACA 65-210 and 64-210 airfoil sections with various type flaps. NACA Rep. 942, 1949.

4. ANSCOMBE, M.A.
RANEY, D.J.
Low-speed tunnel investigation of the effect of body on C_{mo} and aerodynamic centre of unswept wing-body combinations. ARC CP 16, 1950.

5. WEIBERG, J.A.
CAREL, H.C.
Wind-tunnel investigation at low speed of a wing swept back 63° and twisted and cambered for uniform load at a lift coefficient of 0.5 and with a thickened tip section. NACA RM A50I14 (TIL 2559), 1950.

6. JOHNSON, B.H.
SHIBATA, H.H.
Characteristics throughout the subsonic speed range of a plane wing and of a cambered and twisted wing both having 45° of sweepback. NACA RM A51D27 (TIL 2812), 1951.

7. ROSE, L.M.
Low speed characteristics of a wing having 63° sweepback and uniform camber. NACA RM A51D25 (TIL 2781), 1951.

8. SALMI, R.J.
Low speed longitudinal aerodynamic characteristics of a twisted and cambered wing of 45° sweepback and aspect ratio 8, with and without high-lift and stall-control devices and a fuselage at Reynolds numbers from 1.5×10^6 to 4.8×10^6. NACA RM L52C11 (TIL 3192), 1952.

9. BOLTZ, F.W.
SHIBATA, H.H.
Pressure distribution at Mach numbers up to 0.9 on a cambered and twisted wing having 40° of sweepback and an aspect ratio of 10, including the effect of fences. NACA RM A52K20 (TIL 3663), 1953.

10. GRINER, R.F.
Static lateral stability characteristics of an airplane model having a 47.7° sweptback wing of aspect ratio 6 and the contribution of various model components at a Reynolds number of 4.45×10^6. NACA RM L53G09 (TIL 3885), 1953.

11. LETKO, W.
Experimental investigation at low speeds of the effects of wing position on the static stability of models having fuselages of various cross section and unswept and 45° sweptback surfaces. NACA tech. Note 3857, 1956.

12. JAQUET, B.M.
FLETCHER, H.S.
Effects of fuselage nose length and a canopy on the static longitudinal and lateral stability characteristics of 45° sweptback airplane models having fuselages with square cross sections. NACA tech. Note 3961, 1957.

13. PITTS, W.C.
NIELSEN, J.N.
KAATTARI, G.E.
Lift and centre of pressure of wing-body-tail combinations at subsonic, transonic, and supersonic speeds. NACA Rep. 1307, 1957.

14.	HOERNER, S.F.	*Aerodynamic drag*. Published by the author, 1965.
15.	ESDU	Lift-curve slope and aerodynamic centre position of wings in inviscid subsonic flow. Item No. 70011, ESDU International, 1970.
16.	ESDU	Aerodynamic characteristics of aerofoils in compressible inviscid airflow at subcritical Mach numbers. Item No. 72024, ESDU International, 1972.
17.	TORENBEEK, E.	*Synthesis of subsonic aircraft design*. Delft University Press, 1976.
18.	ESDU	Geometric properties of cranked and straight tapered wing planforms. Item No. 76003, ESDU International, 1976.
19.	MORGAN, H.L. PAULSON, J.W.	Aerodynamic characteristics of wing-body configurations with two advanced General Aviation airfoil sections and simple flap systems. NASA tech. Note D-8524, 1977.
20.	ESDU	Wing pitching moment at zero lift at subcritical Mach numbers. Item No. 87001, ESDU International, 1987.
21.	ESDU	Wing angle of attack for zero lift at subcritical Mach numbers. Item No. 87031, ESDU International, 1987.
22.	BAe	Unpublished data.

8.   EXAMPLE

Find the body effect on the wing angle of attack and pitching moment coefficient at zero lift and at low speeds for the wing-body configuration shown in Sketch 8.1. Combine this effect with values for the wing alone to estimate the values for the wing-body combination.

(i)   Definition of geometries

The wing in the example is not straight tapered, so as an initial step the method of Item No. 76003 is applied to the planform geometries of the *exposed* cranked wing to construct an "equivalent" straight-tapered planform, the leading and trailing edges of which are extended to the body centre-line to complete the definition of a gross wing planform for use in the method of this Item. The constructed planform is shown as a heavy dashed outline in Sketch 8.1.

The length of the aerodynamic mean chord and the position of its quarter-chord point are then found and these define the reference chord $\bar{\bar{c}}$ and the moment reference centre. The body planform ahead of a transverse line through this moment reference centre then allows the length l_{Bn} and the area S_{Bn} to be identified.
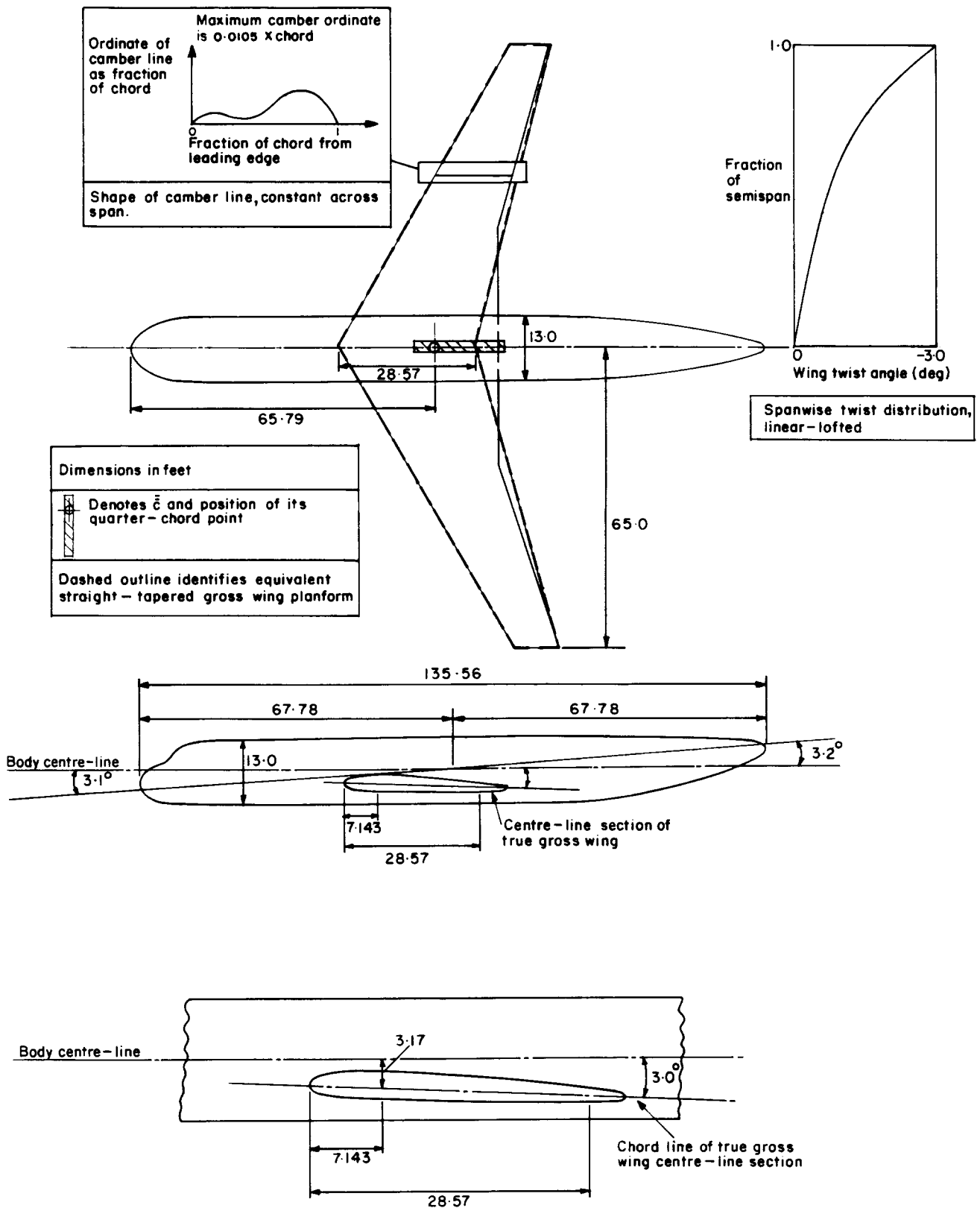
The angle i_W is defined as the angle between the chord line of the true gross wing centre-line section and the centre-line of the body. The wing height z, negative for a low wing, is measured from the body centre-line to the point where the quarter-chord point of the centre-line chord of the equivalent wing would lie on the centre-line chord of the true gross wing.

The geometric properties of the equivalent wing and of the wing-body combination are summarised in Table 8.1.

The shape of the wing section camber line, which in this example is defined to be constant across the span, and the wing twist distribution, which is here defined as linear-lofted with a tip value $\delta_t = -3.0$ deg, are both shown in Sketch 8.1.

TABLE 8.1

Planform properties of equivalent gross wing	*Properties of body and wing-body combination*
b = 130.0 ft $\bar{\bar{c}}$ = 20.36 ft S_W = 2414.1 ft^2 A = 7.0 $\Lambda_{1/4}$ = 25.0 deg $\Lambda_{1/2}$ = 21.3 deg λ = 0.3	h = w = 13.0 ft l_{Bn} = 65.79 ft l_B = 135.56 ft S_{Bn} = 822.6 ft^2 S_B = 1584.2 ft^2 ϕ_a = 3.2 deg ϕ_f = 3.1 deg i_W = 3.0 deg z = –3.17 ft

Sketch 8.1

(ii)   *Estimation of wing-alone zero-lift angle of attack* α_{0rW}

The value of α_{0rW} can be calculated for a wing by the method of Item No. 87031 from a knowledge of the shape of the section camber lines and the spanwise twist distribution. The calculation is made in two parts, the evaluation of the contribution due to the camber of the centre-line section, $(\alpha_{0r})_1$, and of a second contribution due to the combined effects of geometric twist and "camber-dependent" twist. The first contribution, which is needed in its own right in the later calculation of the body effect, is based on an approximate theoretical estimate for two-dimensional flow that is provided by Item No. 72024. That estimate is corrected empirically by multiplication by the constant 0.87. Calculation of the second component involves modelling the twist distribution linearly or by a system of linear segments. Values of the wing planform parameters A and $\Lambda_{1/4}$ are needed in the latter case. A special linear approximation is available for linear-lofted or similar monotonic twist distributions.

The shape of the section camber lines and the spanwise twist distribution in the present example have been chosen to be identical to those assumed in Example 1 of Item No. 87031. For the given camber line Item No. 72024 gives an approximate theoretical two-dimensional value for the zero-lift angle of attack of –1.93 deg, and Item No. 87031 corrects this to a value for the centre-line section

$$(\alpha_{0r})_1 \; = \; 0.87 \times (-1.93) \; = \; -1.68 \text{ deg.}$$

For the given twist distribution the second contribution to α_{0rW} is evaluated in the example of Item No. 87031 as 0.65 deg, so that

$$\alpha_{0rW} \; = \; -1.68 + 0.65 \; = \; -1.03 \text{ deg.}$$

(iii)   *Estimation of body effect on zero-lift angle of attack,* $\Delta\alpha_{0r}$

From Table 8.1, w/b = 13.0/130.0 = 0.1 so that from Equation (3.8), or alternatively from Figure 1,

$$\frac{K_2}{K_1} \; = \; \frac{(1 + 0.7 w/b)}{(1.03 + 2.15 w/b)} \; = \; \frac{(1 + 0.7 \times 0.1)}{(1.03 + 2.15 \times 0.1)} \; = \; 0.859 \, .$$

Therefore Equation (3.6), with angles in degrees, gives

$$\Delta\alpha_{0r} \; = \; \left[1 - \frac{K_2}{K_1}\right]\left[i_W - (\alpha_{0r})_1\right]$$

$$= \; \left[1 - 0.859\right]\left[3 - (-1.68)\right]$$

$$= \; 0.66 \text{ deg.}$$

(iv) *Estimation of wing-body zero-lift angle of attack,* α_{0rWB}

The results of steps (*ii*) and (*iii*) are combined to give

$$\begin{aligned}
\alpha_{0rWB} &= \alpha_{0rW} + \Delta\alpha_{0r} \\
&= -1.03 + 0.66 \\
&= -0.37 \text{ deg.}
\end{aligned}$$

(v) *Estimation of wing-alone pitching-moment coefficient at zero lift,* C_{m0W}

The value of C_{m0W} can be calculated by the method of Item No. 87001 from a knowledge of the shape of the section camber lines, the spanwise twist distribution, and the wing planform parameters A, λ and $\Lambda_{\frac{1}{2}}$. As for α_{0rW}, the calculation is made in two parts. The first involves an evaluation of the overall effect of camber. This is obtained via approximate theoretical estimates of the sectional pitching-moment coefficients at zero lift that are provided by Item No. 72024. These are then modified by two empirical factors that correct for the approximations involved in those estimates and allow for planform effects. The second part involves an evaluation of the combined effects of geometric and "camber-dependent" twist.

The shape of the camber line in the present example is the same as that in Example 1 of Item No. 87001. For that shape Item No. 72024 gives an approximate theoretical two-dimensional value of –0.0589 for the zero-lift pitching-moment coefficient. Item No. 87001 applies two correction factors to that value. In the case of constant camber shape, as here, the first correction is by a single factor that depends on the size of the theoretical approximation. In other cases a carefully devised averaging process that involves the wing taper λ would be carried out by considering corrected values for the sections at 20% and 80% of the wing semispan. The second correction factor is a function of A and $\Lambda_{\frac{1}{2}}$ that allows for remaining planform effects. For the constant camber shape in Sketch 8.1, and planform parameters $A = 7$ and $\Lambda_{\frac{1}{2}} = 21.3$ deg, Example 1 of Item No. 87001 evaluates the part of C_{m0W} due to camber as –0.0446.

The part of C_{m0W} that is due to the twist distribution is evaluated in Item No. 87001 as a function of the planform parameters λ, A and $\Lambda_{\frac{1}{4}}$ and of the effective twist angles at 20% and 80% of the wing semispan. For the twist distribution in Sketch 8.1 (which is not the same as that in Example 1 of Item No. 87001) and with $\lambda = 0.3$, $A = 7$ and $\Lambda_{\frac{1}{4}} = 25$ deg, a contribution to C_{m0W} of +0.0114 is estimated.

Therefore, for the wing alone the total value is

$$C_{m0W} = -0.0446 + 0.0114 = -0.0332 .$$

(vi) *Estimation of body effect on pitching-moment coefficient at zero lift,* ΔC_{m0}

From the dimensions in Sketch 8.1 and Table 8.1,

$$w^2/S_B = 13.0^2/1584.2 = 0.107 ,$$

and

$$\frac{S_{Bn}l_{Bn}}{S_B l_B} = \frac{822.6 \times 65.79}{1584.2 \times 135.56} = 0.252 .$$

For these values Figure 2 gives

$$\frac{10^3 (C_{m0})_B S_W \bar{\bar{c}}}{\psi S_B l_B} = -1.35 \ \text{deg}^{-1}.$$

For the present example, the forebody and afterbody angles, as defined in Sketch 4.1, have the values $\phi_f = 3.1$ deg and $\phi_a = 3.2$ deg.

Therefore from Equation (4.5), with all angles in degrees,

$$\psi = i_W - \alpha_{0rW} + \phi_f - 0.6\phi_a$$

$$= 3 - (-1.03) + 3.1 - 0.6 \times 3.2$$

$$= 5.21 \ \text{deg}.$$

Thus $(C_{m0})_B = -0.00135 S_B l_B \psi / S_W \bar{\bar{c}}$

$$= -0.00135 \times 1584.2 \times 135.56 \times 5.21/(2414.1 \times 20.36)$$

$$= -0.0307.$$

From Equation (4.2), with $z/h = -3.17/13.0 = -0.244$, the contribution due to wing height is

$$\Delta_z C_{m0} = 0.01(z/h)$$

$$= 0.01 \times (-0.244)$$

$$= -0.0024.$$

And from Equation (4.3), with $\delta_t = -3.0$ deg, $w/b = 0.10$, $A = 7.0$ and $\Lambda_{1/4} = 25.0$ deg, the contribution due to wing sweep is

$$\Delta_s C_{m0} = -0.053[(C_{m0})_B \delta_t (w/b) A \tan \Lambda_{1/4}]^{0.3}$$

$$= -0.053[(-0.0307) \times (-3.0) \times (0.1) \times 7.0 \times \tan 25°]^{0.3}$$

$$= -0.0185.$$

Therefore, the total effect of the body is

$$\Delta C_{m0} = (C_{m0})_B + \Delta_z C_{m0} + \Delta_s C_{m0}$$

$$= -0.0307 - 0.0024 - 0.0185$$

$$= -0.0516.$$

(vii)   *Estimation of wing-body pitching-moment coefficient at zero lift, C_{m0WB}*

The results of steps (*v*) and (*vi*) are combined to give

$$
\begin{aligned}
C_{m0WB} \;=\;& C_{m0W} + \Delta C_{m0} \\
=\;& -0.0332 - 0.0516 \\
=\;& -0.085 \,.
\end{aligned}
$$

(viii)   *Summary*

For the configuration in the example the body effects are:-

$$\Delta \alpha_{0r} = 0.66 \ \text{deg and} \ \Delta C_{m0} = -0.052 \,.$$

The wing-alone values are:-

$$\alpha_{0rW} = -1.03 \ \text{deg and} \ C_{m0W} = -0.033 \,.$$

The values for the wing-body configuration are:-

$$\alpha_{0rWB} = -0.37 \ \text{deg and} \ C_{m0WB} = -0.085 \,.$$

Although the calculation has been performed for a camber shape that is constant across the wing span and for a linear-lofted twist distribution the methods in Item Nos 87001 and 87031 are fully capable of dealing with more general cases, and the methods for estimating the body effects remain compatible.
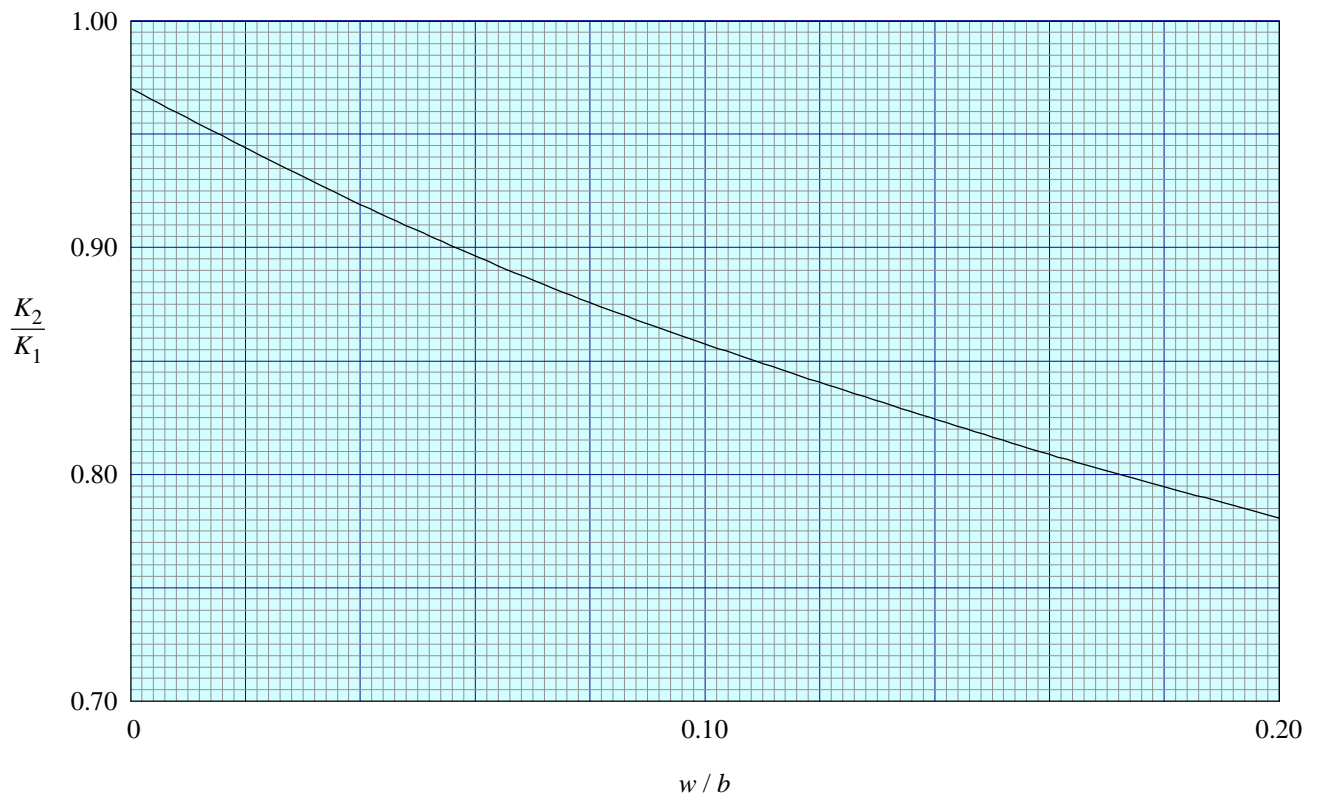
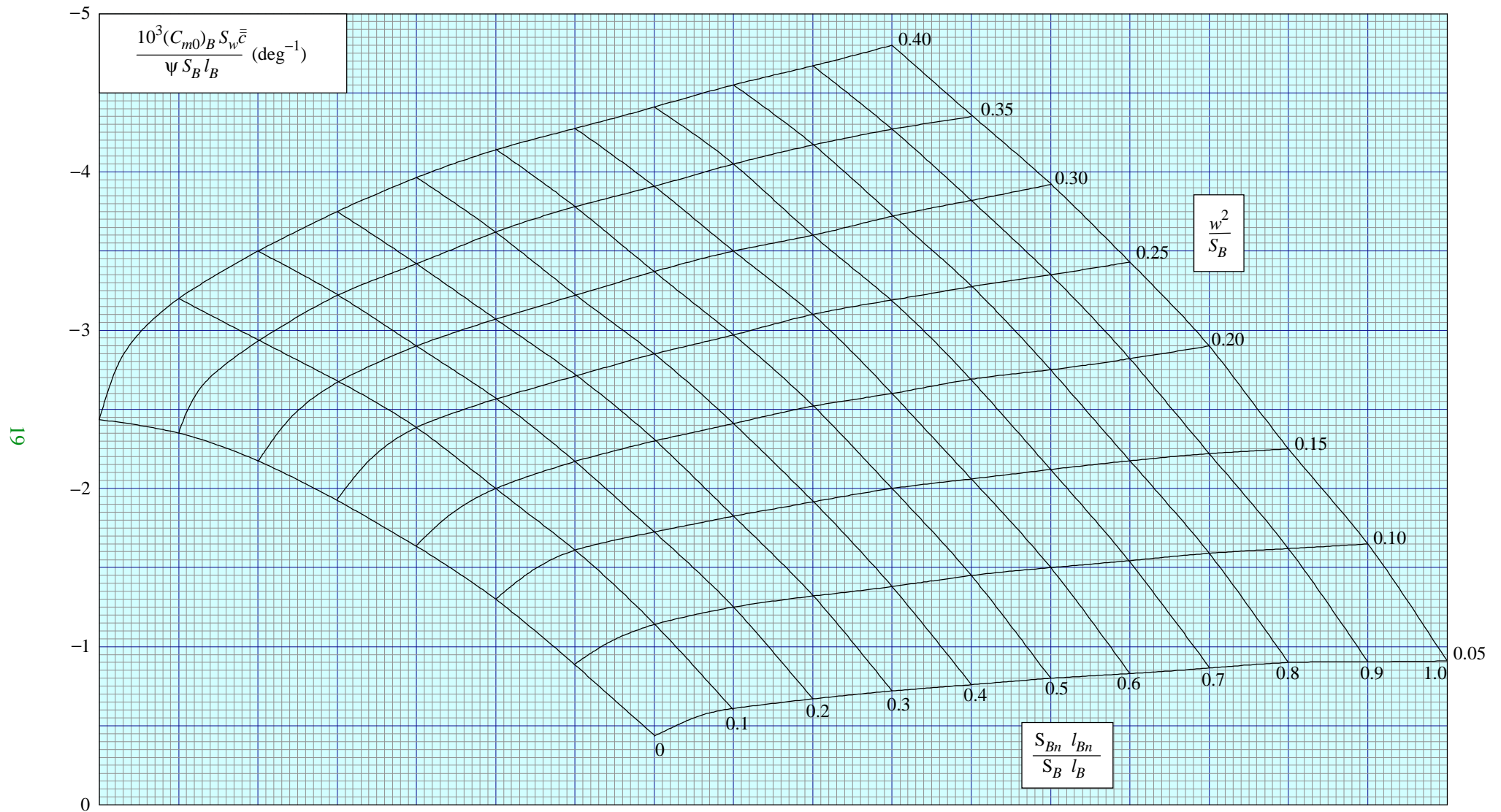**FIGURE 1 RATIO OF SLENDER-BODY FACTORS**

$$\frac{10^3 (C_{m0})_B S_w \bar{\bar{c}}}{\psi S_B l_B} \ (\text{deg}^{-1})$$

$$\frac{w^2}{S_B}$$

$$\frac{S_{Bn}}{S_B} \frac{l_{Bn}}{l_B}$$

FIGURE 2 BODY EFFECT ON ZERO-LIFT PITCHING-MOMENT COEFFICIENT FOR UNSWEPT WINGS AT MID-BODY HEIGHT

THE PREPARATION OF THIS DATA ITEM

The work on this particular Data Item, which supersedes Item No. Aero A.08.01.07 was monitored and guided by the Aerodynamics Committee, which first met in 1942 and now has the following membership:

Chairman
Mr H.C. Garner   – Independent

Vice-Chairman
Mr P.K. Jones   – British Aerospace (Commercial Aircraft) Ltd, Woodford

Members
Mr G.E. Bean[*]   – Boeing Aerospace Company, Seattle, Wash., USA
Dr N.T. Birch   – Rolls-Royce plc, Derby
Mr K. Burgin   – Southampton University
Dr T.J. Cummings   – Short Brothers plc
Mr J.R.J. Dovey   – Independent
Mr L. Elmeland[*]   – Saab-Scania, Linköping, Sweden
Dr J.W. Flower   – Independent
Dr K.P. Garry   – Cranfield Institute of Technology
Mr P.G.C. Herring   – Sowerby Research Centre, Bristol
Mr R. Jordan   – Aircraft Research Association
Mr J.H. Kraus[*]   – Northrop Corporation, Hawthorne, Calif., USA
Mr J.R.C. Pedersen   – Independent
Mr R. Sanderson   – Messerschmitt-Bölkow-Blohm GmbH, Bremen, Germany
Mr A.E. Sewell[*]   – McDonnell Douglas, Long Beach, Calif., USA
Mr M.R. Smith   – British Aerospace (Commercial Aircraft) Ltd, Bristol
Miss J. Willaume   – Aérospatiale, Toulouse, France.

[*] Corresponding Members

The technical work in the assessment of the available information and the construction and subsequent development of the Data Item was undertaken by

Mr J. Henley-King   – Engineer.

The person with overall responsibility for the work in this subject area is Mr P.D. Chappell, Head of the Aircraft Aerodynamics Group.